Fungal Automata

Andrew Adamatzky[1]
Eric Goles[1,2]
Genaro J. Martínez[1,3]
Michail-Antisthenis Tsompanas[1]
Martin Tegelaar[4]
Han A. B. Wosten[4]

[1] *Unconventional Computing Laboratory, UWE, Bristol, UK*
[2] *Faculty of Engineering and Science, University Adolfo Ibáñez, Santiago, Chile*
[3] *High School of Computer Science, National Polytechnic Institute, Mexico*
[4] *Microbiology Department, University of Utrecht, Utrecht, The Netherlands*

We study a cellular automaton (CA) model of information dynamics on a single hypha of a fungal mycelium. Such a filament is divided in compartments (here also called cells) by septa. These septa are invaginations of the cell wall and their pores allow for the flow of cytoplasm between compartments and hyphae. The septal pores of the fungal phylum of the Ascomycota can be closed by organelles called Woronin bodies. Septal closure is increased when the septa become older and when exposed to stress conditions. Thus, Woronin bodies act as informational flow valves. The one-dimensional fungal automaton is a binary-state ternary neighborhood CA, where every compartment follows one of the elementary cellular automaton (ECA) rules if its pores are open and either remains in state 0 (first species of fungal automata) or its previous state (second species of fungal automata) if its pores are closed. The Woronin bodies closing the pores are also governed by ECA rules. We analyze a structure of the composition space of cell-state transition and pore-state transition rules and the complexity of fungal automata with just a few Woronin bodies, and exemplify several important local events in the automaton dynamics.

Keywords: fungi; ascomycete; Woronin body; cellular automata

1. Introduction

The fungal kingdom represents organisms colonizing all ecological niches [1], where they play a key role [2–5]. Fungi can consist of a single cell, can form enormous underground networks [6] and can form microscopic fruit bodies or fruit bodies weighing up to half a ton [7]. The underground mycelium network can be seen as a distributed

https://doi.org/10.25088/ComplexSystems.29.4.759

communication and information processing system linking together trees, fungi and bacteria [8]. Mechanisms and dynamics of information processing in mycelium networks form an unexplored field, with just a handful of papers published related to space exploration by mycelia [9, 10], patterns of electrical activity of fungi [11–13] and potential use of fungi as living electronic and computing devices [14–16].

Filamentous fungi grow by means of hyphae that grow at their tip and that branch subapically. Hyphae may be coenocytic or divided in compartments by septa. Filamentous fungi in the phylum Ascomycota have porous septa that allow for cytoplasmic streaming [17, 18]. Woronin bodies plug the pores of these septa after hyphal wounding to prevent excessive bleeding of cytoplasm [19–24]. In addition, they plug septa of intact growing hyphae to maintain intra- and inter-hyphal heterogeneity [25–28].

Woronin bodies can be located in different hyphal positions (Figure 1(a)). When first formed, Woronin bodies are generally localized to the apex [29–31]. Subsequently, Woronin bodies are either transported to the cell cortex (*Neurospora crassa*, *Sordaria fimicola*) or to the septum (*Aspergillus oryzae*, *Aspergillus nidulans*, *Aspergillus fumigatus*, *Magnaporthe grisea*, *Fusarium oxysporum*, *Zymoseptoria tritici*), where they are anchored with a leashin tether and largely immobile until they are translocated to the septal pore due to cytoplasmic flow or ATP depletion [23–30, 32–35]. Woronin bodies that are not anchored at the cellular cortex or the septum are located in the cytoplasm and are highly mobile (*Aspergillus fumigatus*, *Aspergillus*

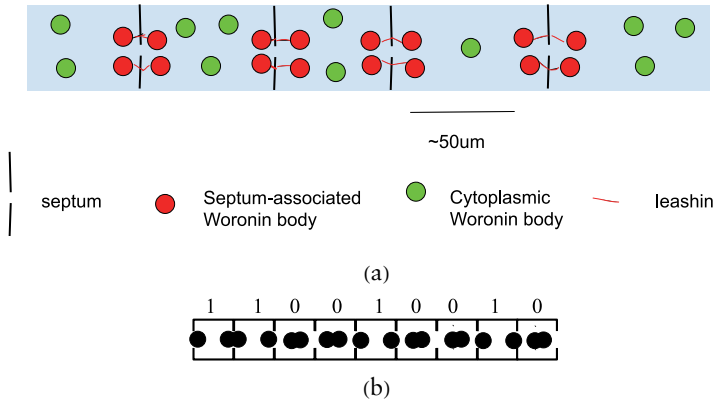

Figure 1. (a) A biological scheme of a fragment of a fungal hypha of an ascomycete, where we can see septa and associated Woronin bodies. (b) A scheme representing states of Woronin bodies: 0 open, 1 closed.

nidulans, *Zymoseptoria tritici*) [27, 29, 31]. Septal pore occlusion can be induced by bulk cytoplasmic flow [27] or developmental [36] and environmental cues, like puncturing of the cell wall, high temperature, carbon and nitrogen starvation, high osmolarity and low pH. Interestingly, high environmental pH reduces the proportion of occluded apical septal pores [28].

Aiming to lay a foundation of an emerging paradigm of fungal intelligence—distributed sensing and information processing in living mycelium networks—we decided to develop a formal model of the mycelium and investigate the role of Woronin bodies in potential information dynamics in the mycelium.

The paper is structured as follows. We introduce fungal automata in Section 2. Properties of the composition of cell state transition and Woronin body state transition functions are studied in Section 3. The complexity of space-time configuration of fungal automata, where just a few cells have Woronin bodies, is studied in Section 4. Section 5 exemplifies local events, which could be useful for computation with fungal automata, happening in fungal automata with sparsely but regularly positioned cells with Woronin bodies. The paper concludes with Section 6.

2. Fungal Automata $\mathcal{M}$

A fungal automaton is a one-dimensional cellular automaton with binary cell states and ternary, including central cell, cell neighborhood, governed by two elementary cellular automaton (ECA) rules, namely the cell state transition rule f and the Woronin bodies adjustment rule g: $\mathcal{M} = \langle \mathbf{N}, u, \mathbf{Q}, f, g \rangle$. Each cell x_i has a unique index $i \in \mathbf{N}$. Its state is updated from $\mathbf{Q} = \{0, 1\}$ in discrete time depending on its current state x_i^t, the states of its left x_{i-1}^t and right x_{i+1}^t neighbors and the state of cell x's Woronin body w. Woronin bodies take states from $\mathbf{Q}$: $w^t = 1$ means Woronin bodies (Figure 1) in cell x block the pores and the cell has no communication with its neighbors, and $w^t = 0$ means that Woronin bodies in cell x do not block the pores. Woronin bodies update their states $g(\cdot)$, $w^{t+1} = g\big(u(x)^t\big)$, depending on the state of the neighborhood $u(x)^t$. Cells x update their states by function $f(\cdot)$ if their Woronin bodies do not block the pores.

Two species of mycelium automata are considered: $\mathcal{M}_1$, where each cell updates its state as follows:

$$x^{t+1} = \begin{cases} 0 & \text{if } w^t = 1 \\ f\big(u(x)^t\big) & \text{otherwise} \end{cases}$$

https://doi.org/10.25088/ComplexSystems.29.4.759

and $\mathcal{M}_2$, where each cell updates its state as follows:

$$x^{t+1} = \begin{cases} x^t & \text{if } w^t = 1 \\ f\big(u(x)^t\big) & \text{otherwise} \end{cases}$$

where $w^t = g\big(u(x)^t\big)$.

State 1 in the cells of array x symbolizes metabolites, signals exchanged between cells. Where pores in a cell are open, the cell updates its state by ECA rule $f : \{0, 1\}^3 \to \{0, 1\}$.

In automaton $\mathcal{M}_1$, when Woronin bodies block the pores in a cell, the cell does not update its state and remains in the state 0, and left and right neighbors of the cells cannot detect any "cargo" in this cell. In automaton $\mathcal{M}_2$, where Woronin bodies block the pores in a cell, the cell does not update its state and remains in its current state. In a real living mycelium, glucose and possibly other metabolites [26] can still cross the septum even when septa are closed by Woronin bodies, but we can ignore this fact in the present abstract model.

Both species are biologically plausible and thus will be studied in parallel. The rules for closing and opening Woronin bodies are also ECA rules $g : \{0, 1\}^3 \to \{0, 1\}$. If $g\big(u(x)^t\big) = 0$, this means that pores are open, if $g\big(u(x)^t\big) = 1$, Woronin bodies block the pores. Examples of space-time configurations of both species of $\mathcal{M}$ are shown in Figure 2.

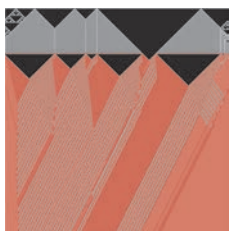

(a) $\mathcal{M}_1$, $\rho_f =$ 133, \n$\rho_g$=116

(b) $\mathcal{M}_2$, $\rho_f =$ 133, \n$\rho_g$=116

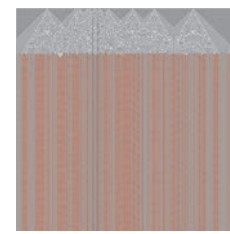

(c) $\mathcal{M}_1$, $\rho_f = 73$, $\rho_g = 128$

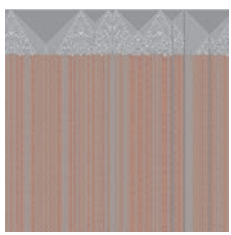

(d) $\mathcal{M}_2$, $\rho_f = 73$, $\rho_g = 128$

(e) $\mathcal{M}_1$, $\rho_f = 61$, $\rho_g = 132$

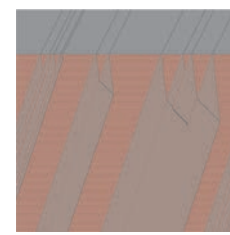

(f) $\mathcal{M}_2$, $\rho_f = 61$, $\rho_g = 132$

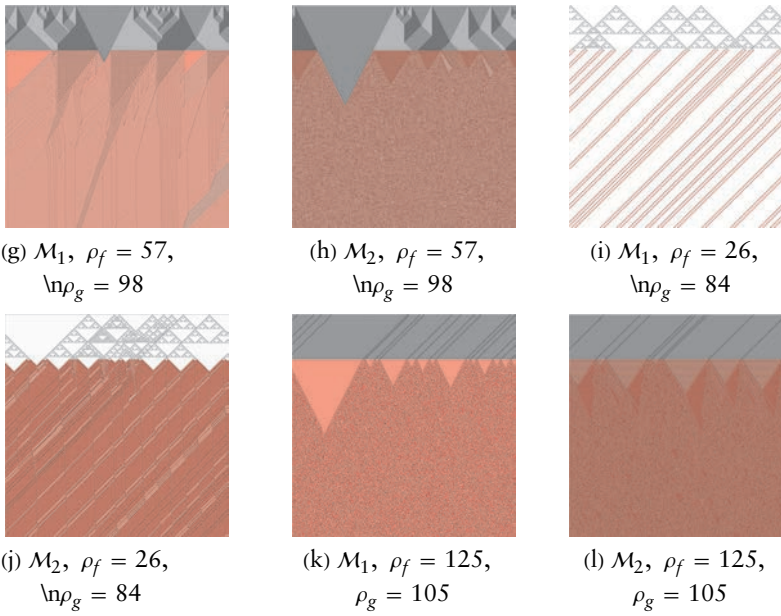

(g) $\mathcal{M}_1$, $\rho_f = 57$, $\backslash n\rho_g = 98$ (h) $\mathcal{M}_2$, $\rho_f = 57$, $\backslash n\rho_g = 98$ (i) $\mathcal{M}_1$, $\rho_f = 26$, $\backslash n\rho_g = 84$

(j) $\mathcal{M}_2$, $\rho_f = 26$, $\backslash n\rho_g = 84$ (k) $\mathcal{M}_1$, $\rho_f = 125$, $\rho_g = 105$ (l) $\mathcal{M}_2$, $\rho_f = 125$, $\rho_g = 105$

Figure 2. Examples of space-time dynamics of $\mathcal{M}$. The automata are 10^3 cells each. Initial configuration is random with probability of a cell x to be in state 1, $x^0 = 1$ equal to 0.01. Each automaton evolved for 10^3 iterations. Binary values of ECA rules f and g are shown in subcaptions. Rule g is applied to every iteration starting from the 200^{th}. Cells in state 0 are white, in state 1 are black and cells with Woronin bodies blocking pores are red. Indexes of cells increase from the left to the right; iterations increase from the top to the bottom.

3. Properties of Composition $f \circ g$

Predecessor Sets

Let $\mathbf{F} = \left\{h : \{0, 1\}^3 \to \{0, 1\}\right\}$ be a set of all ECA functions. Then any composition $f \circ g$, where $f, g \in \mathbf{F}$, can be converted to a single function $h \in \mathbf{F}$. For each $h \in \mathbf{F}$ we can construct a set $\mathbf{P}(h) = \left\{f \circ g \in \mathbf{F} \times \mathbf{F} \mid f \circ g \to h\right\}$. The sets $\mathbf{P}(h)$ for each $h \in \mathbf{F}$ are available online: https://figshare.com/s/b7750ee3fe6df7cbe228.

A size of $\mathbf{P}(h)$ for each h is shown in Figure 3(c). The functions with the largest size of $\mathbf{P}(h)$ are rule 0 in automaton $\mathcal{M}_1$ and rule 51 in $\mathcal{M}_2$ (only neighborhood configurations 010, 011, 110, 111 are mapped into 1).

https://doi.org/10.25088/ComplexSystems.29.4.759

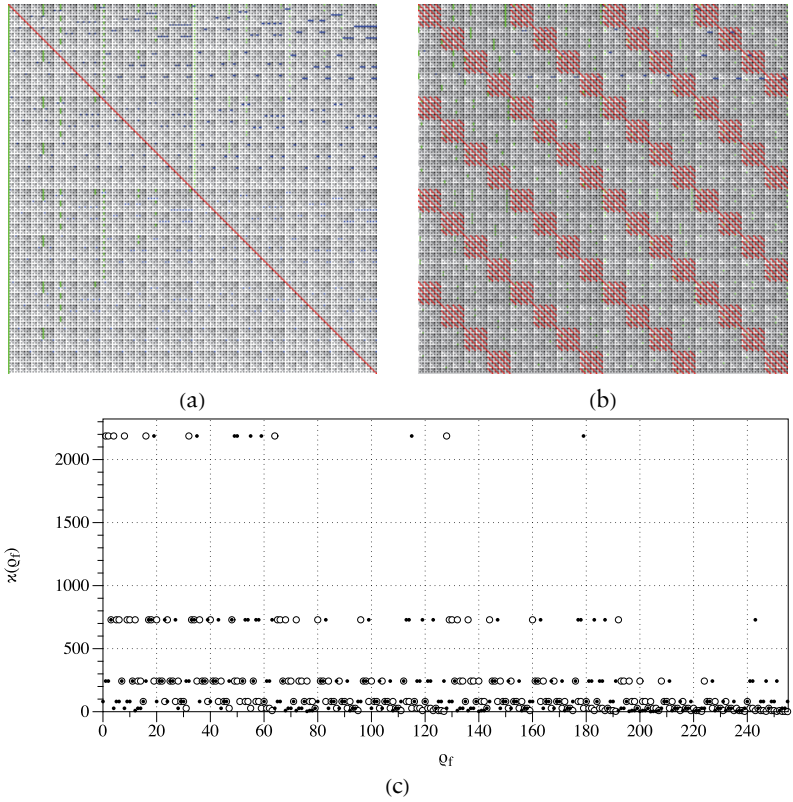

Figure 3. Mapping $\mathbf{F}\times\mathbf{F} \to \mathbf{F}$ for automata (a) $\mathcal{M}_1$ and (b) $\mathcal{M}_2$ is visualized as an array of pixels, $\mathbf{P} = (p)_{0\le\rho_f\le255,\,0\le\rho_f\le255}$. An entry at the intersection of any ρ_f and ρ_g is colored as follows: red if $p_{\rho_f\rho_g} = p_{\rho_g\rho_f}$, blue if $\rho_g = p_{\rho_g\rho_f}$, green if $\rho_f = p_{\rho_g\rho_f}$. (c) Sizes of $\mathbf{P}(h)$ sets for $\mathcal{M}_1$, circle and $\mathcal{M}_2$, solid disks are shown for every function h apart from rule 0 ($\mathcal{M}_1$) and rule 51 ($\mathcal{M}_2$).

Size σ of $\mathbf{P}(h)$ versus a number γ of functions h having set $\mathbf{P}(h)$ of size σ is shown for automata $\mathcal{M}_1$ and $\mathcal{M}_2$ in Table 1(a).

With regard to Wolfram classification [37], sizes of $\mathbf{P}(h)$ for rules from class III vary from 9 to 729 in $\mathcal{M}_1$ (Table 1(b)). Rule 126 would be the most difficult to obtain in $\mathcal{M}_1$ by the composition of two ECA rules chosen at random; it has only nine "predecessor" $f\circ g$ pairs. Rule 18 would be the easiest to obtain for class III rules; it has 729 predecessors, in both $\mathcal{M}_1$ (Table 1(b)) and $\mathcal{M}_2$ (Table 1(d)). In $\mathcal{M}_1$, one rule, rule 41, from the class IV has 243 $f\circ g$ predecessors, and all other rules in that class have 81 (Table 1(c)). From class IV, rule 54

has the largest number of predecessors in $\mathcal{M}_2$, and thus can be considered as most common (Table 1(d)).

(a) Rules per $|\mathbf{P}(h)|$

σ	γ
1	1
3	8
9	28
27	56
81	70
243	56
729	28
2187	8
6561	1

(b) $\mathcal{M}_1$: Class III rules

Rule	σ
18	729
22, 146	243
30, 45, 60, 90, 105, 150	81
122	27
126	9

(c) $\mathcal{M}_1$: Class IV rules

Rule	σ
41	243
54, 106, 110	81

(d) $\mathcal{M}_2$: Class III rules

Rule	σ
18	729
22, 146	243
30, 45, 60 90, 105, 150	81
122	243
126	81

(e) $\mathcal{M}_2$: Class IV rules

Rule	σ
41	243
54	729
106	81
110	27

Table 1. Characterizations of automaton mapping $\mathbf{F}\times\mathbf{F} \to \mathbf{F}$. (a) Size σ of $\mathbf{P}(h)$ versus a number γ of functions h having set $\mathbf{P}(h)$ of size σ. Size of sets $\mathbf{P}(h)$ for rules of automaton $\mathcal{M}_1$ from Wolfram (b) class III, (c) class IV, and automaton $\mathcal{M}_2$ from Wolfram class (d) III and (e) IV.

Diagonals

In automaton $\mathcal{M}_1$, for any $f \in \mathbf{F}$, $f \circ f = 0$. Assume $f : \{0, 1\}^3 \to 1$, then Woronin bodies close the pores and thus, a second application of f produces state 0. If $f : \{0, 1\}^3 \to 0$, then Woronin bodies do not close pores but yet a second application of the f produces state 0.

For automaton $\mathcal{M}_2$, a structure of diagonal mapping $f \circ f \to h$, where $f, h \in \mathbf{F}$, is shown in Table 2. The set of the diagonal outputs $f \circ f$ consists of 16 rules: (0, 1, 2, 3), (16, 17, 18, 19), (32, 33, 34, 35), (48, 49, 40, 51). This set of rules can be reduced to the following rule. Let

$$C(x^t) = \left[u(x)^t = (111)\right] \vee \left[u(x)^t = (111)\right]$$

https://doi.org/10.25088/ComplexSystems.29.4.759

and

$$B(x^t) = \left[u(x)^t = (011)\right] \vee \left[u(x)^t = (010)\right].$$

Then $x^t = 1$ if $C(x)^t \vee C(x)^t \wedge B(x^t)$.

$f \circ f$	f
0	0, 1, 2, 3, 16, 17, 18, 19, 32, 33, 34, 35, 48, 49, 50, 51
1	128, 129, 130, 131, 144, 145, 146, 147, 160, 161, 162, 163, 176, 177, 178, 179
2	64, 65, 66, 67, 80, 81, 82, 83, 96, 97, 98, 99, 112, 113, 114, 115
3	192, 193, 194, 195, 208, 209, 210, 211, 224, 225, 226, 227, 240, 241, 242, 243
16	8, 9, 10, 11, 24, 25, 26, 27, 40, 41, 42, 43, 56, 57, 58, 59
17	136, 137, 138, 139, 152, 153, 154, 155, 168, 169, 170, 171, 184, 185, 186, 187
18	72, 73, 74, 75, 88, 89, 90, 91, 104, 105, 106, 107, 120, 121, 122, 123
19	200, 201, 202, 203, 216, 217, 218, 219, 232, 233, 234, 235, 248, 249, 250, 251
32	4, 5, 6, 7, 20, 21, 22, 23, 36, 37, 38, 39, 52, 53, 54, 55
33	132, 133, 134, 135, 148, 149, 150, 151, 164, 165, 166, 167, 180, 181, 182, 183
34	68, 69, 70, 71, 84, 85, 86, 87, 100, 101, 102, 103, 116, 117, 118, 119
35	196, 197, 198, 199, 212, 213, 214, 215, 228, 229, 230, 231, 244, 245, 246, 247
48	12, 13, 14, 15, 28, 29, 30, 31, 44, 45, 46, 47, 60, 61, 62, 63
49	140, 141, 142, 143, 156, 157, 158, 159, 172, 173, 174, 175, 188, 189, 190, 191
50	76, 77, 78, 79, 92, 93, 94, 95, 108, 109, 110, 111, 124, 125, 126, 127
51	204, 205, 206, 207, 220, 221, 222, 223, 236, 237, 238, 239, 252, 253, 254, 255

Table 2. Diagonals of automaton $\mathcal{M}_2$.

Commutativity

In automaton $\mathcal{M}_1$, for any $f, g \in \mathrm{F}$, $f \circ g \neq g \circ f$ only if $f \neq g$. In automaton $\mathcal{M}_2$ there are 32 768 pairs of functions where $\circ$ is commutative, their distribution visualized in red in Figure 3(b).

Identities and Zeros

In automaton $\mathcal{M}_1$, there are no left or right identities, or right zeros in $\langle \mathrm{F}, \mathrm{F}, \circ \rangle$. The only left zero is the rule 0. In automaton $\mathcal{M}_2$, there are no identities or zeros at all.

Associativity

In automaton $\mathcal{M}_1$, there are 456 976 triples $\langle f, g, h\rangle$ for which operation $\circ$ is associative: $(f \circ g) \circ h = f \circ (g \circ h)$. The ratio of associative triples to the total number of triples is 0.027237892. There are 104 976 associative triples in $\mathcal{M}_2$, a ratio of 0.006257057.

4. Tuning Complexity: Rule 110

To evaluate how introduction of Woronin bodies could affect the complexity of automaton evolution, we undertook two series of experiments. In the first series we used a fungal automaton where just one cell has a Woronin body (Figure 4). In the second series we employed a fungal automaton where regularly positioned cells (but not all cells of the array) have Woronin bodies.

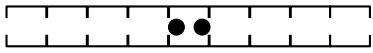

Figure 4. Only one cell has has two Woronin bodies by which it can close itself off from the other compartments.

State transition functions g of Woronin bodies were varied but the state transition function f of a cell was rule 110, $\rho_f = 110$. We have chosen rule 110 because the rule is proven to be computationally universal [38, 39] and P-complete [40]. The rule belongs to Wolfram class IV, renowned for exhibiting complex and nontrivial interactions between traveling localizations [41]. Rich families of gliders can be produced in collisions with other gliders [42–44].

We wanted to check how an introduction of Woronin bodies affects the dynamics of a rule 110 automaton. Thus, we evolved the automata from all possible initial configurations of eight cells placed near the end of an $n = 1000$ cell array of resting cells and allowed to evolve for 950 iterations. Lempel–Ziv (LZ) complexity (compressibility) was evaluated via sizes of space-time configurations saved as PNG files. This is sufficient because the "deflation" algorithm used in PNG lossless compression [45–47] is a variation of the classical Lempel–Ziv 1977 algorithm [48]. Estimates of LZ complexity for each of the eight-cell initial configurations are shown in Figure 5(a). The initial configurations with the highest estimated LZ complexity are 10110001 (decimal 177), 11010001 (209), 10000011 (131), 11111011 (253); see the example of space-time dynamics in Figure 5(b).

https://doi.org/10.25088/ComplexSystems.29.4.759

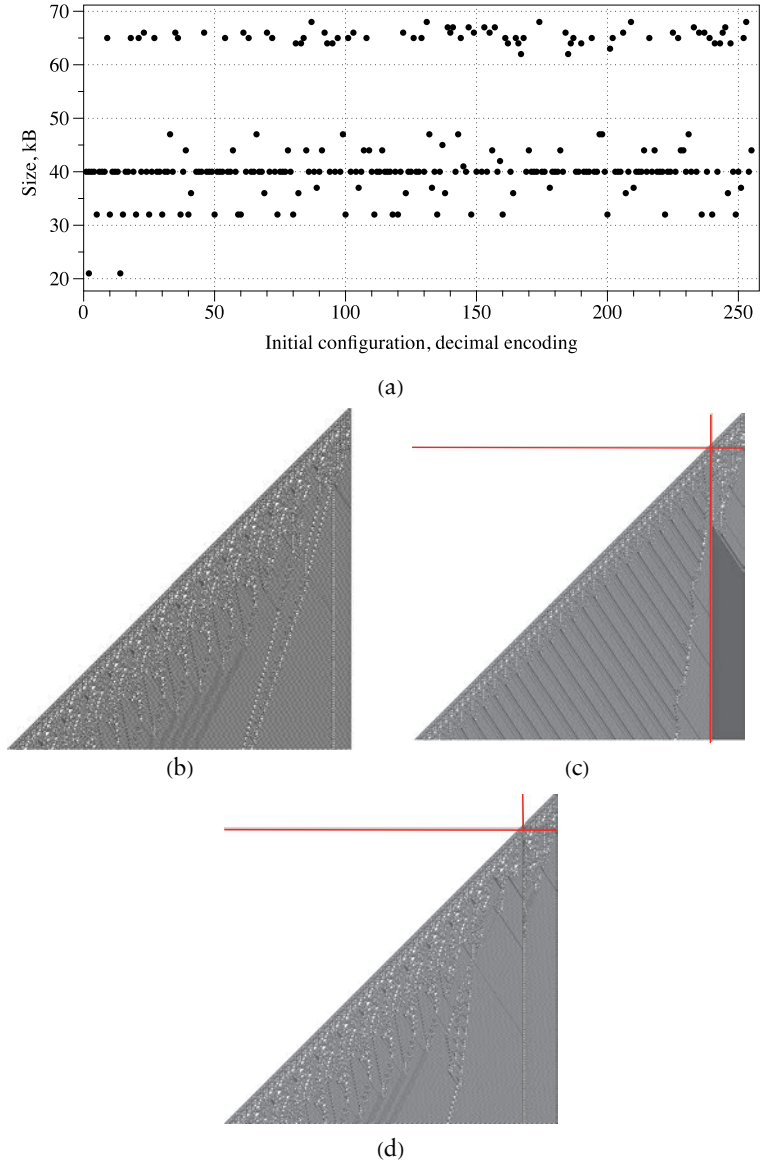

Figure 5. (a) Estimates of LZ complexity of space-time configurations of ECA rule 110 without Woronin bodies. (b) A space-time configuration of ECA rule 110 evolving from initial configuration 10110001 (177); no Woronin bodies are activated. (c) A space-time configuration of $\mathcal{M}_1$ rule 110 evolving from initial configuration 10110001 (177). (d) Woronin body is governed by rule 43. Red lines indicate the time when the body was activated and the position of the cell with the body. In (bcd), a pixel in position (i, t) is black if $x_i^t = 1$.

We assumed that a cell in the position $n - 100$ has a Woronin body that can be activated (Figure 4), that is, start updating its state by rule f, after the 100^{th} iteration of the automaton evolution. We then ran 950 iterations of automaton evolution for each of 256 Woronin rules and estimated LZ complexity. In experiments with $\mathcal{M}_1$, we found that 128 rules with even decimal representations do not affect the space-time dynamics of evolution, and 128 rules with even decimal representations reduce the complexity of the space-time configuration. The key reasons for the complexity reduction (compare Figure 5(b) and (c)) are cancellation of three gliders after 300 iterations and simplification of the behavior of glider guns positioned at the tail of the propagating wavefront. In experiments with $\mathcal{M}_2$, 128 rules with even decimal representations do not change the space-time configuration. The other 128 rules reduce complexity and modify the space-time configuration by rearranging the structures of the glider guns and establishing one oscillator at the site surrounding the position of the cell with the Woronin body (Figure 5(d)).

In the second series of experiments, we regularly positioned cells with Woronin bodies along the one-dimensional array: every 50^{th} cell has a Woronin body. Then we evolved fungal automata $\mathcal{M}_1$ and $\mathcal{M}_2$ from exactly the same initial random configuration with a density of 1 equal to 0.3. The space-time configuration of the automaton without Woronin bodies is shown in Figure 6(a). Exemplars of space-time configurations of automata with Woronin bodies are shown in Figure 6(b–h). As seen in Figure 7, both species of fungal automata show similar dynamics of complexity along the Woronin transition functions ordered by their decimal values. The automaton $\mathcal{M}_1$ has average LZ complexity 82.2 ($\overline{\sigma} = 24.6$) and the automaton $\mathcal{M}_2$ has 78.4 ($\overline{\sigma} = 22.1$). Woronin rules g that generate most LZ complex space-time configurations are $\rho_g = 133$ in $\mathcal{M}_1$ (Figure 6(b)) and $\rho_g = 193$ in $\mathcal{M}_2$ (Figure 6(e)). The space-time dynamics of the automaton is characterized by a substantial number of glider guns and gliders (Figure 6(b)). Functions in the middle of the descending hierarchy of LZ complexity produce space-time configurations with a declined number of traveling localizations and growing domains of homogeneous states (Figure 6(cg)). Automata with Woronin functions at the bottom of the complexity hierarchy quickly (i.e., after 200 to 300 iterations) evolve toward stable equilibrium states (Figure 6(dh)).

https://doi.org/10.25088/ComplexSystems.29.4.759

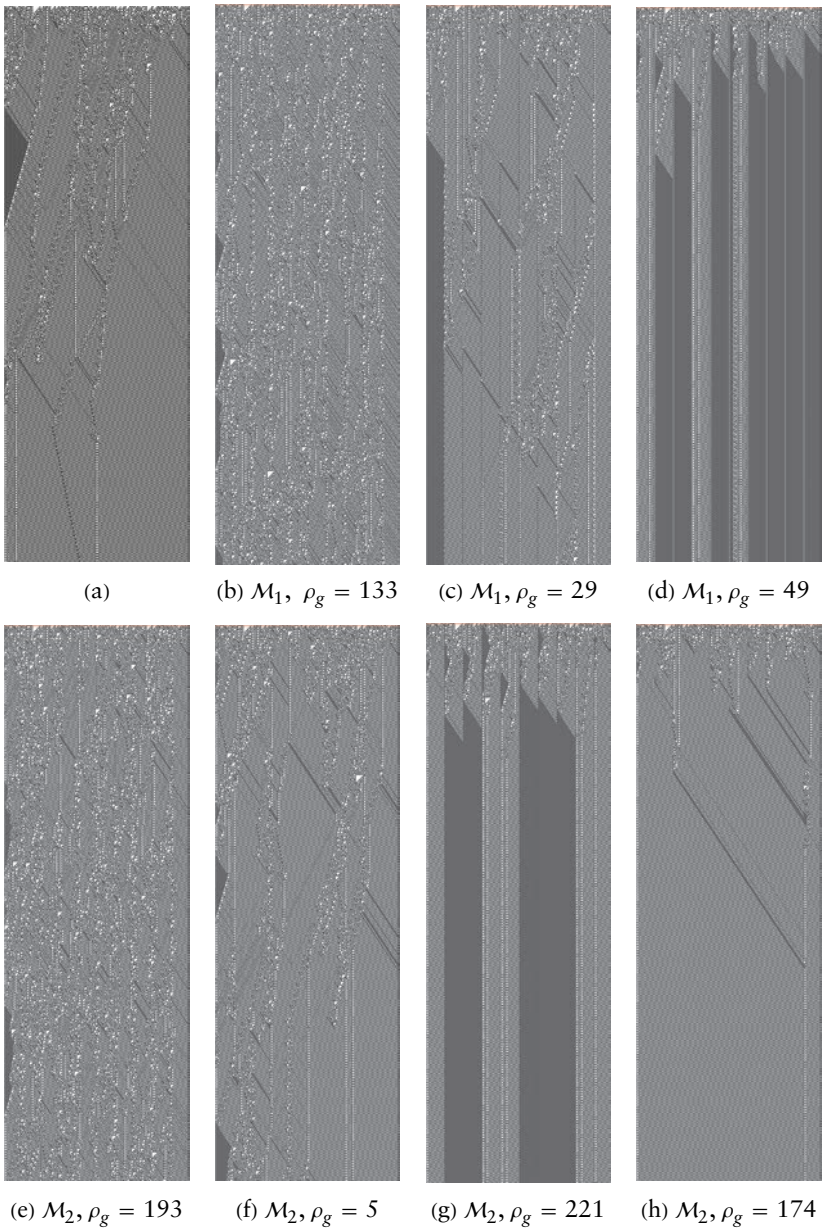

Figure 6. (a) ECA rule 110, no Woronin bodies. Space-time evolution of (bcd) $\mathcal{M}_1$ and (e–h) $\mathcal{M}_2$ for Woronin rules shown in subcaption. LZ complexity of space-time configurations decreases from (b) to (d) and from (e) to (h). Every 50^{th} cell has a Woronin body.

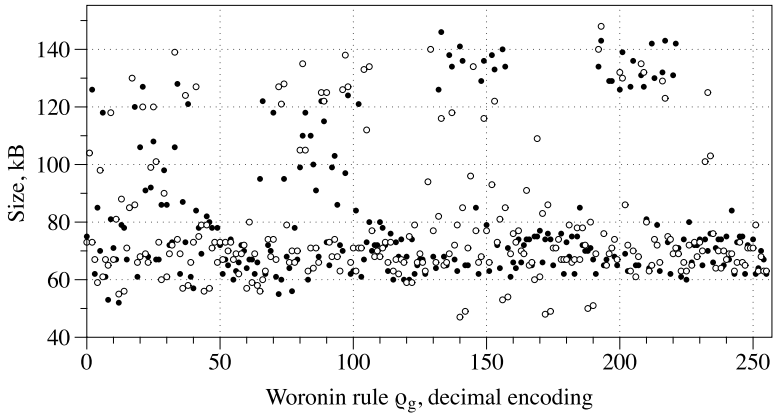

Figure 7. Estimations of LZ complexity of space-time, 500 cells by 500 iterations, configurations of $\mathcal{M}_1$, circle and $\mathcal{M}_2$, solid disks, for all Woronin functions g.

5. Local Events

Let us consider some local events happening in the fungal automata discussed in Section 4: every 50^{th} cell of an array has a Woronin body.

Retaining gliders. A glider can be stopped and converted into a stationary localization by a cell with a Woronin body. As exemplified in Figure 8(a), the localization traveling left was stopped from further propagation by a cell with a Woronin body, yet the localization did not annihilate but remained stationary.

Register memory. Different substrings of the input string (initial configuration) might lead to different equilibrium configurations achieved in the domains of the array separated by cells with Woronin bodies. When there are just two types of equilibrium configurations, they can be seen as "bit up" and "bit down" and therefore such a fungal automaton can be used as a memory register (Figure 8(b)).

Reflectors. In many cases, cells with Woronin bodies induce local domains of stationary, sometimes time oscillations, inhomogeneities that might act as reflectors for traveling localizations. An example is shown in Figure 8(c), where several localizations are repeatedly bouncing between two cells with Woronin bodies.

Modifiers. Cells with Woronin bodies can act as modifiers of states of gliders reflected from them and of outcomes of collision between traveling localizations. In Figure 8(d) we can see how a traveling localization is reflected from the vicinity of Woronin bodies three times: every time the state of the localization changes. On the third reflection, the localization becomes stationary. In the fragment (Figure 8(e))

https://doi.org/10.25088/ComplexSystems.29.4.759

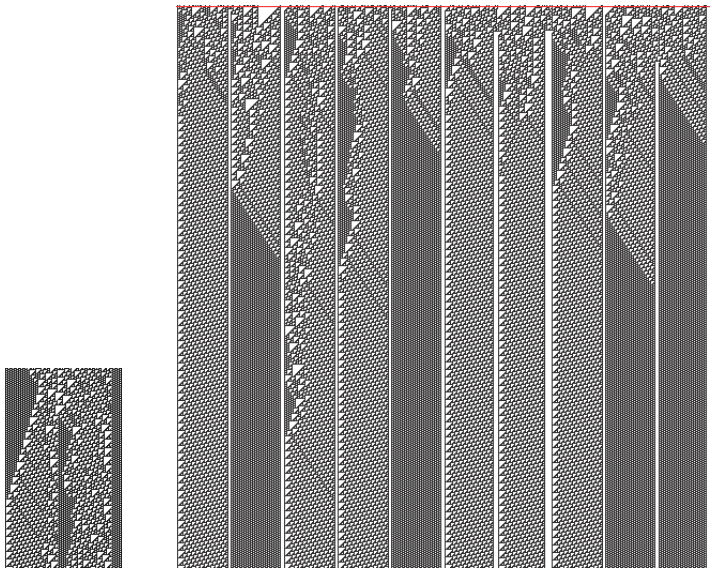

(a) $\mathcal{M}_1,\ \rho_g = 2$ (b) $\mathcal{M}_1,\ \rho_g = 15$

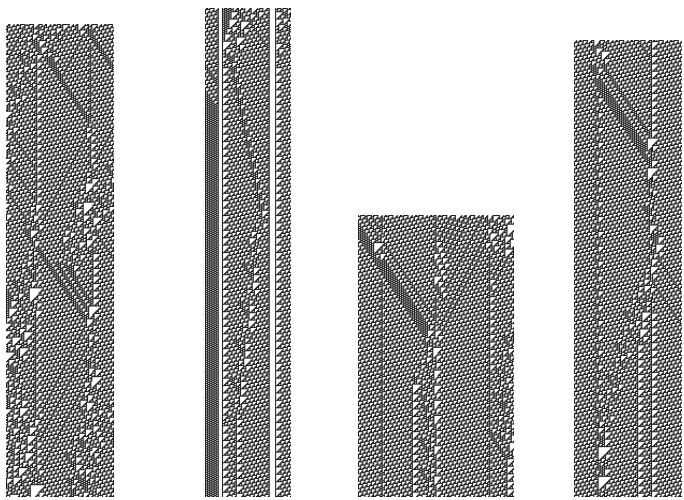

(c) $\mathcal{M}_1, \rho_g = 21$ (d) $\mathcal{M}_1, \rho_g = 31$ (e) $\mathcal{M}_1, \rho_g = 29$ (f) $\mathcal{M}_1, \rho_g = 201$

Figure 8. (a) Localization traveling left was stopped by the Woronin body. (b) Analog of a memory register. (c) Reflections of traveling localizations from cells with Woronin bodies. (d) Modification of glider state in the vicinity of Woronin bodies. (e) A fragment of configuration of automaton with $\rho_g = 29$, left cell states, right Woronin bodies states. (f) Enlarged subfragment of the fragment (d) where a Wonorin body tunes the outcome of the collision. For both automata $\rho_f = 110$.

of the space-time configuration of an automaton with Woronin bodies governed by $\rho_g = 201$ of the fragment, we can see how two localizations got into contact with each other in the vicinity of the Woronin body and an advanced structure is formed. Two breathing stationary localizations act as a mirror, and there are streams of traveling localizations between them. A multistep chain reaction can be observed in Figure 8(f): there are two stationary, breathing localizations at the sites of the cells with Woronin bodies. A glider is formed on the left stationary localization. The glider travels to the right and collides into the right breather. In the result of the collision, the breather undergoes structural transitions, emits a glider traveling left and transforms itself into a pair of stationary breathers. Meanwhile the newly born glider collides into the left breather and changes its state.

6. Discussion

As a first step toward formalization of fungal intelligence, we introduced one-dimensional fungal automata operated by two local transition functions: one, g, governs states of Woronin bodies (pores are open or closed); another, f, governs cell states: 0 and 1. We provided a detailed analysis of the magma $\langle f, g, \circ \rangle$, results of which might be useful for future designs of computational and language recognition structures with fungal automata. The magma as a whole does not satisfy any other property but closure. Chances are high that there are subsets of the magma that might satisfy conditions of other algebraic structures. A search for such subsets could be one of the topics of further studies.

Another topic could be an implementation of computational circuits in fungal automata. For certain combinations of f and g we can find quite sophisticated families of stationary and traveling localizations and many outcomes of the collisions and interactions between these localizations; an illustration is shown in Figure 9. Thus the target could be, for example, to construct an n-binary full adder that is as compact in space and time as possible.

The theoretical results reported show that by controlling just a few cells with Woronin bodies it is possible to drastically change the dynamics of the automaton array. A third direction of future studies could be in implemented information processing in a single hypha. In such a hypothetical experimental setup, input strings would be represented by arrays of illumination and outputs could be patterns of electrical activity recorded from the mycelium hypha resting on an electrode array.

https://doi.org/10.25088/ComplexSystems.29.4.759

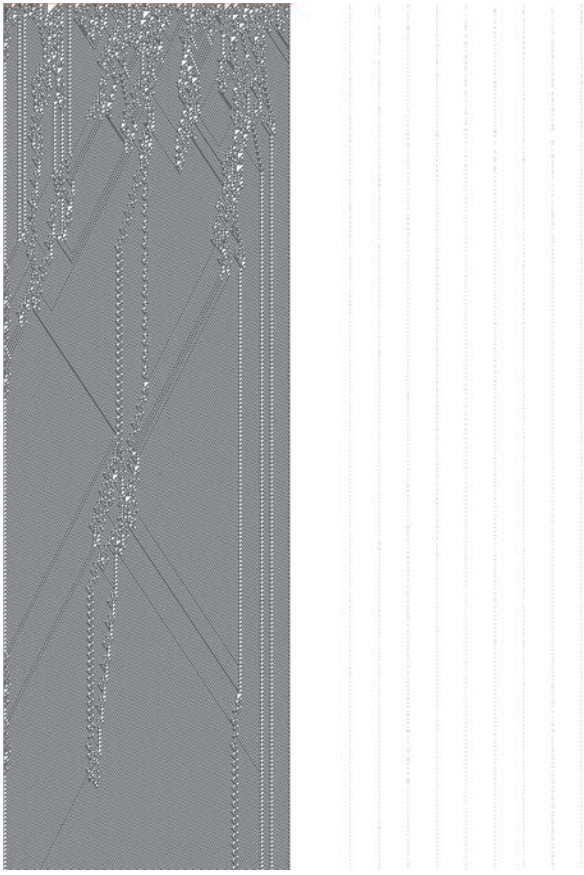

Figure 9. An example of 5-inputs-7-outputs collision in $\mathcal{M}_2$, $\rho_f = 110$, $\rho_g = 40$. Every 50^{th} cell has a Woronin body. Cell state transitions are shown on the left, Woronin bodies state transitions on the right. A pixel in position (i, t) is black if $x_i^t = 1$, left or $w_i^t = 1$, right.

Acknowledgments

A. Adamatzky, M. Tegelaar and H. A. B. Wosten have received funding from the European Union's Horizon 2020 research and innovation programme FET OPEN "Challenging current thinking" under grant agreement Number 858132. E. Goles's residency in UWE has been supported by funding from the Leverhulme Trust under the Visiting Research Professorship grant VP2-2018-001.

References

[1] M. J. Carlile, S. C. Watkinson and G. W. Gooday, *The Fungi*, 2nd ed., San Diego, CA: Academic Press, 2001.

[2] D. M. Griffin et al., *Ecology of Soil Fungi*, London: Chapman and Hall, 1972.

[3] R. C. Cooke and A. D. M. Rayner, *Ecology of Saprotrophic Fungi*, New York: Longman, 1984.

[4] A. D. M. Rayner and L. Boddy, *Fungal Decomposition of Wood: Its Biology and Ecology*, New York: Wiley, 1988.

[5] M. Christensen, "A View of Fungal Ecology," *Mycologia*, **81**(1), 1989 pp. 1–19. doi:10.1080/00275514.1989.12025620.

[6] M. L. Smith, J. N. Bruhn and J. B. Anderson, "The Fungus *Armillaria bulbosa* Is among the Largest and Oldest Living Organisms," *Nature*, **356**(6368), 1992 pp. 428–431. doi:10.1038/356428a0.

[7] Y.-C. Dai and B.-K. Cui, "*Fomitiporia ellipsoidea* has the Largest Fruiting Body among the Fungi," *Fungal Biology*, **115**(9), 2011 pp. 813–814. doi:10.1016/j.funbio.2011.06.008.

[8] P. Bonfante and I.-A. Anca, "Plants, Mycorrhizal Fungi, and Bacteria: A Network of Interactions," *Annual Review of Microbiology*, **63**(1), 2009 pp. 363–383. doi:10.1146/annurev.micro.091208.073504.

[9] M. Held, C. Edwards and D. V. Nicolau, "Fungal Intelligence; or on the Behaviour of Microorganisms in Confined Micro-environments," in *Journal of Physics: Conference Series*, **178**, 012005. IOP Publishing, 2009. doi:10.1088/1742-6596/178/1/012005.

[10] M. Held, C. Edwards and D. V. Nicolau, "Examining the Behaviour of Fungal Cells in Microconfined Mazelike Structures," in *Imaging, Manipulation, and Analysis of Biomolecules, Cells, and Tissues VI*, San Jose, CA (D. L. Farkas, D. V. Nicolau and R. C. Leif, eds.), Bellingham, WA: International Society for Optics and Photonics, 2008 68590U. doi:10.1117/12.759453.

[11] C. L. Slayman, W. S. Long and D. Gradmann, " 'Action Potentials' in *Neurospora crassa*, a Mycelial Fungus," *Biochimica et Biophysica Acta (BBA)-Biomembranes*, **426**(4), 1976 pp. 732–744. doi:10.1016/0005-2736(76)90138-3.

[12] S. Olsson and B. S. Hansson, "Action Potential-like Activity Found in Fungal Mycelia Is Sensitive to Stimulation," *Naturwissenschaften*, **82**(1), 1995 pp. 30–31. doi:10.1007/BF01167867.

[13] A. Adamatzky, "On Spiking Behaviour of Oyster Fungi *Pleurotus djamor*," *Scientific Reports*, **8**, 2018 7873. doi:10.1038/s41598-018-26007-1.

[14] A. Adamatzky, "Towards Fungal Computer," *Interface Focus*, **8**(6), 2018 20180029. doi:10.1098/rsfs.2018.0029.

[15] A. Adamatzky, M. Tegelaar, H. A. B. Wosten, A. L. Powell, A. E. Beasley and R. Mayne, "On Boolean Gates in Fungal Colony." arxiv.org/abs/2002.09680.

[16] A. E. Beasley, M.-S. Abdelouahab, R. Lozi, A. L. Powell and A. Adamatzky, "Mem-fractive Properties of Mushrooms." arxiv.org/abs/2002.06413.

[17] R. T. Moore and J. H. McAlear, "Fine Structure of Mycota. 7. Observations on Septa of Ascomycetes and Basidiomycetes," *American Journal of Botany*, **49**(1), 1962 pp. 86–94. doi:10.1002/j.1537-2197.1962.tb11750.x.

[18] R. R. Lew, "Mass Flow and Pressure-Driven Hyphal Extension in *Neurospora crassa*," *Microbiology*, **151**(8), 2005 pp. 2685–2692. doi:10.1099/mic.0.27947-0.

[19] A. P. J. Trinci and A. J. Collinge, "Occlusion of the Septal Pores of Damaged Hyphae of *Neurospora crassa* by Hexagonal Crystals," *Protoplasma*, **80**(1), 1974 pp. 57–67. doi:10.1007/BF01666351.

[20] A. J. Collinge and P. Markham, "Woronin Bodies Rapidly Plug Septal Pores of Severed *Penicillium chrysogenum* Hyphae," *Experimental Mycology*, **9**(1), 1985 pp. 80–85. doi:10.1016/0147-5975(85)90051-9.

[21] G. Jedd and N. H. Chua, "A New Self-Assembled Peroxisomal Vesicle Required for Efficient Resealing of the Plasma Membrane," *Nature Cell Biology*, **2**(4), 2000 pp. 226–231. doi:10.1038/35008652.

[22] K. Tenney, I. Hunt, J. Sweigard, J. I. Pounder, C. McClain, E. J. Bowman and B. J. Bowman, "*hex-1*, a Gene Unique to Filamentous Fungi, Encodes the Major Protein of the Woronin Body and Functions as a Plug for Septal Pores," *Fungal Genetics and Biology*, **31**(3), 2000 pp. 205–217. doi:10.1006/fgbi.2000.1230.

[23] S. Soundararajan, G. Jedd, X. Li, M. Ramos-Pamploña, N. H. Chua and N. I. Naqvi, "Woronin Body Function in *Magnaporthe grisea* Is Essential for Efficient Pathogenesis and for Survival during Nitrogen Starvation Stress," *The Plant Cell*, **16**(6), 2004 pp. 1564–1574. doi:10.1105/tpc.020677.

[24] J.-ichi Maruyama, P. R. Juvvadi, K. Ishi and K. Kitamoto, "Three-Dimensional Image Analysis of Plugging at the Septal Pore by Woronin Body during Hypotonic Shock Inducing Hyphal Tip Bursting in the Filamentous Fungus *Aspergillus oryzae*," *Biochemical and Biophysical Research Communications*, **331**(4), 2005 pp. 1081–1088. doi:10.1016/j.bbrc.2005.03.233.

[25] R.-J. Bleichrodt, G. J. van Veluw, B. Recter, J.-ichi Maruyama, K. Kitamoto and H. A. B. Wösten, "Hyphal Heterogeneity in *Aspergillus oryzae* Is the Result of Dynamic Closure of Septa by Woronin Bodies," *Molecular Microbiology*, **86**(6), 2012 pp. 1334–1344. doi:10.1111/mmi.12077.

[26] R.-J. Bleichrodt, M. Hulsman, H. A. B. Wösten and M. J. T. Reinders, "Switching from a Unicellular to Multicellular Organization in an *Aspergillus niger* Hypha," *MBio*, **6**(2), 2015 e00111–15. doi:10.1128/mbio.00111-15.

[27] G. Steinberg, N. J. Harmer, M. Schuster and S. Kilaru, "Woronin Body-Based Sealing of Septal Pores," *Fungal Genetics and Biology*, **109**, 2017 pp. 53–55. doi:10.1016/j.fgb.2017.10.006.

[28] M. Tegelaar, R.-J. Bleichrodt, B. Nitsche, A. F. J. Ram and H. A. B. Wösten, "Subpopulations of Hyphae Secrete Proteins or Resist Heat Stress in *Aspergillus oryzae* Colonies," *Environmental Microbiology*, **22**(1), 2020 pp. 447–455. doi:10.1111/1462-2920.14863.

[29] M. Momany, E. A. Richardson, C. Van Sickle and G. Jedd, "Mapping Woronin Body Position in *Aspergillus nidulans*," *Mycologia*, **94**(2), 2002 pp. 260–266. doi:10.1080/15572536.2003.11833231.

[30] W. K. Tey, A. J. North, J. L. Reyes, Y. F. Lu and G. Jedd, "Polarized Gene Expression Determines Woronin Body Formation at the Leading Edge of the Fungal Colony," *Molecular Biology of the Cell*, **16**(6), 2005 pp. 2651–2659. doi:10.1091/mbc.E04-10-0937.

[31] J. Beck and F. Ebel, "Characterization of the Major Woronin Body Protein HexA of the Human Pathogenic Mold *Aspergillus fumigatus*," *International Journal of Medical Microbiology*, **303**(2), 2013 pp. 90–97. doi:10.1016/j.ijmm.2012.11.005.

[32] S. K. Ng, F. Liu, J. Lai, W. Low and G. Jedd, "A Tether for Woronin Body Inheritance Is Associated with Evolutionary Variation in Organelle Positioning," *PLoS Genetics*, **5**(6), 2009 e1000521. doi:10.1371/journal.pgen.1000521.

[33] W. P. Wergin, "Development of Woronin Bodies from Microbodies in *Fusarium oxysporum f. sp. lycopersici*," *Protoplasma*, **76**(2), 1973 pp. 249–260. doi:10.1007/BF01280701.

[34] Y. Leonhardt, S. C. Kakoschke, J. Wagener and F. Ebel, "Lah is a Transmembrane Protein and Requires Spa10 for Stable Positioning of Woronin Bodies at the Septal Pore of *Aspergillus fumigatus*," *Scientific Reports*, **7**(1), 2017 44179. doi:10.1038/srep44179.

[35] M. W. Berns, J. R. Aist, W. H. Wright and H. Liang, "Optical Trapping in Animal and Fungal Cells Using a Tunable, Near-Infrared Titanium-Sapphire Laser," *Experimental Cell Research*, **198**(2), 1992 pp. 375–378. doi:10.1016/0014-4827(92)90395-O.

[36] R.-J. Bleichrodt, A. Vinck, N. D. Read and H. A. B. Wösten, "Selective Transport between Heterogeneous Hyphal Compartments via the Plasma Membrane Lining Septal Walls of *Aspergillus niger*," *Fungal Genetics and Biology*, **82**, 2015 pp. 193–200. doi:10.1016/j.fgb.2015.06.010.

[37] S. Wolfram, *Cellular Automata and Complexity: Collected Papers*, Reading, MA: Addison-Wesley Publishing Company, 1994.

[38] K. Lindgren and M. G. Nordahl, "Universal Computation in Simple One-Dimensional Cellular Automata," *Complex Systems*, **4**(3), 1990 pp. 299–318. complex-systems.com/pdf/04-3-4.pdf.

[39] M. Cook, "Universality in Elementary Cellular Automata," *Complex Systems*, **15**(1), 2004 pp. 1–40. complex-systems.com/pdf/15-1-1.pdf.

[40] T. Neary and D. Woods, "P-Completeness of Cellular Automaton Rule 110," in *Automata, Languages and Programming (ICALP 2006)*, Venice, Italy, 2006 (M. Bugliesi, B. Preneel, V. Sassone and I. Wegener, eds.), Berlin, Heidelberg: Springer, 2006 pp. 132–143. doi:10.1007/11786986_13.

[41] S. Wolfram, "Universality and Complexity in Cellular Automata," *Physica D: Nonlinear Phenomena*, **10**(1–2), 1984 pp. 1–35. doi:10.1016/0167-2789(84)90245-8.

[42] G. J. Martínez, H. V. McIntosh and J. C. Seck-Tuoh Mora, "Production of Gliders by Collisions in Rule 110," in *Advances in Artificial Life (ECAL 2003)*, Dortmund, Germany, 2003 (W. Banzhaf, J. Ziegler, T. Christaller, P. Dittrich and J. T. Kim, eds.), Berlin, Heidelberg: Springer, 2003 pp. 175–182. doi:10.1007/978-3-540-39432-7_19.

[43] G. J. Martínez, H. V. McIntosh and J. C. Seck-Tuoh Mora, "Gliders in Rule 110," *International Journal of Unconventional Computing*, **2**(1), 2006 1.

[44] G. J. Martínez, H. V. McIntosh, J. C. Seck-Tuoh Mora and S. V. C. Vergara, "Rule 110 Objects and Other Collision-Based Constructions," *Journal of Cellular Automata*, **2**(3), 2007 pp. 219–242.

[45] G. Roelofs, *PNG: The Definitive Guide*, Sebastopol, CA: O'Reilly & Associates, Inc., 1999.

[46] P. G. Howard, *The Design and Analysis of Efficient Lossless Data Compression Systems*, Ph.D. thesis, Brown University, Providence, RI, 1993.

[47] P. Deutsch and J.-L. Gailly, "Zlib Compressed Data Format Specification Version 3.3," Technical report, 1996. datatracker.ietf.org/doc/rfc1950.

[48] J. Ziv and A. Lempel, "A Universal Algorithm for Sequential Data Compression," *IEEE Transactions on Information Theory*, **23**(3), 1977 pp. 337–343. doi:10.1109/TIT.1977.1055714.